Three-dimensional Langevin calculations of fission fragment mass-energy distribution from excited compound nuclei

A. V. Karpov,[1] P. N. Nadtochy,[1] D. V. Vanin,[2] and G. D. Adeev[1]
[1]*Omsk State University, Department of Theoretical Physics, Mira Prospekt 55-A, Omsk RU-644077, Russia*
[2]*Flerov Laboratory of Nuclear Reactions, Joint Institute for Nuclear Research, Dubna RU-141980, Russia*
(Received 16 August 2000; published 18 April 2001)

A stochastic approach to fission dynamics based on three-dimensional Langevin equations was applied to calculate fission fragment mass-energy distribution from a number of excited compound nuclei formed in reactions induced by heavy ions. Evaporation of prescission light particles along Langevin fission trajectories from the ground state of the compound nucleus to its scission has been taken into account using a Monte Carlo simulation technique. Inclusion of the third collective coordinate in Langevin dynamics leads to a considerable increase of the variance of the mass and the kinetic-energy distributions of fission fragments as compared with two-dimensional Langevin calculations. A liquid-drop model with finite range of nuclear forces and a modified one-body mechanism for nuclear dissipation have been used in the calculations. The results of the calculations are compared with the available experimental data. The calculations performed using the three-dimensional Langevin dynamics reproduce sufficiently well all the parameters of the two-dimensional fission fragment mass-energy distribution and their dependence on various parameters of the compound nucleus. The mean prescission neutron multiplicities are also reproduced with good accuracy. In order to reproduce simultaneously the measured prescission neutron multiplicities and the variance of the fission fragment mass-energy distribution, the reduction coefficient of the contribution from a wall formula has to be decreased at least by half of the one-body dissipation strength ($0.25 \leqslant k_s \leqslant 0.5$).

DOI: 10.1103/PhysRevC.63.054610 PACS number(s): 25.85.−w, 02.50.Ey, 05.10.Gg

I. INTRODUCTION

During the last two decades a stochastic approach [1–4] based on the multidimensional Fokker-Planck equation (FPE) [5–8] or on the set of multidimensional Langevin equations, which is equivalent [9] to the multidimensional FPE, has been extensively and rather successfully used to solve many problems of collective nuclear dynamics in such reactions as fusion-fission, deep-inelastic heavy-ion collisions, induced fission, and quasifission (see reviews [3–6] and references therein). Almost all the problems of collective nuclear dynamics are essentially multidimensional, but the multidimensional FPE can be solved only using approximate methods [5–8], while numerical solution of the equivalent system of Langevin equations is possible nearly without any approximations. Therefore, although at the beginning of the 1980s application of the stochastic approach to nuclear dynamics was based mainly on the FPE, an obvious preference has been given recently to the Langevin equations [3,4]. It should be noted that the computation time and the amount of calculation increase extremely fast with the increasing number of collective coordinates in the Langevin equations. Because of this the stochastic approach based on the Langevin equations had not been applied so far in its full extent to study the characteristics of induced fission. Up to now only one-dimensional [4,10] and two-dimensional [11–16] Langevin calculations have been carried out. The latter makes it possible to calculate the mass and the kinetic-energy distributions of fission fragments, as well as the mean prescission neutron multiplicities and fission probability, whereas the main subject of the one-dimensional calculations [4,10] is only the analysis of the mean prescission multiplicity of light particles and fission probability. But even in the two-dimensional Langevin calculations the problem of the mass and the kinetic-energy distributions was solved [11–16] only in a restricted form. First, attention was paid to computation of only the first and second moments of the distributions. Second, these were the parameters of the one-dimensional distributions. The kinetic-energy distribution was computed [11–14] for symmetric fission, whereas the mass distribution corresponded to the most probable kinetic energy. Furthermore, the correlation of the parameters of these distributions was ignored.

The characteristics of the experimentally observed two-dimensional mass-energy distribution (MED) of fission fragments are usually discussed in terms of the first and second moments of the one-dimensional distribution, which can be obtained from the two-dimensional MED of fission fragments by integration over the proper parameter. Consequently, the theoretical approaches used to interpret the experimental data, including the Langevin dynamics, should also guarantee the possibility of computation of the fission fragment MED and, on the basis of this distribution, the one-dimensional fission fragment mass and kinetic-energy distributions and their moments. So far, the two-dimensional MED of fission fragments has been investigated sufficiently fully for the first time in the studies of Nix and Swiatecki in their dynamical model [17] with zero viscosity, and later by Adeev and co-workers [6,18] in the framework of a diffusion model based on the multidimensional FPE. In addition to the possibility of adequate comparison with the experimental data, the theoretical investigation of the two-dimensional MED of fission fragments is of great interest from the point of view of studying correlation of the distribution parameters. The correlation of the fission fragment masses and ki-

netic energies contains additional information about scission configuration of the fissioning nucleus.

In the present paper we report the results of systematic calculations of the fission fragment MED performed using the stochastic approach based on the three-dimensional Langevin equations. It should be mentioned that qualitative estimations of the influence that the third collective coordinate (mass asymmetry coordinate) in the Langevin dynamics exerts on the parameters of the fission fragment kinetic-energy distribution, as well as some computational results, were first presented in Ref. [3], but a systematic study of the two-dimensional MED of fission fragments had not been done there.

The purpose of the paper is to study fission dynamics consistently from the ground state of the compound nucleus to its scission under discrete cooling due to evaporation of light prescission particles and to calculate the mean multiplicities of these particles, particularly of neutrons, as well as the parameters of the two-dimensional MED of fission fragments. We hope to draw some conclusions about the dissipation mechanism of nuclear collective motion in fission of excited nuclei by comparison of the theoretically calculated values of the observable quantities with the experimental data. Our research in this paper is restricted to a fission of sufficiently excited nuclei formed in reactions of complete fusion in the entrance channel of reactions. Our model needs further development for reactions of quasifission (fast fission). A detailed description of dynamics in the entrance channel of the reactions is necessary. The paper is organized as follows: the model and basic equations are described in Sec. II; the calculations and numerical results are discussed in Sec. III; finally, the concluding remarks are given in Sec. IV.

II. THE MODEL AND BASIC EQUATIONS

A. Parametrization of nuclear surface and collective coordinates

A felicitous parametrization of the shape of a fissioning nucleus is very important when investigating its dynamical evolution. Optimal for our purposes is the well-known [19,20] ''funny hills'' parametrization $\{c,h,\alpha\}$. Actually, in our dynamical calculations we used a slightly modified form of the $\{c,h,\alpha\}$ parametrization. This conveniently provides a three-parametric family of shapes that have been employed in numerous studies of static [19,20] as well as dynamical [6,13–15] characteristics of fissioning nuclei. It was shown [19,20] that this simple parametrization describes with rather a good quantitative accuracy the properties of the saddle point shapes obtained in liquid-drop model (LDM) calculations, where practically no restrictions were imposed on nuclear shapes [21,22].

In cylindrical coordinates the surface of the nucleus is given by

$$\rho_s^2(z)=\begin{cases} c^{-2}(c^2-z^2)\left(A_s c^2+Bz^2+\dfrac{\alpha' z}{c^2}\right), & B\geqslant 0 \\ c^{-2}(c^2-z^2)\left(A_s c^2+\dfrac{\alpha' z}{c^2}\right)\exp(Bcz^2), & B<0, \end{cases} \tag{1}$$

where z is the coordinate along the symmetry axis and ρ_s is the radial coordinate of the nuclear surface. In Eq. (1) the quantities A_s and B are defined by means of the shape parameters as

$$B=2h+\frac{c-1}{2},$$

$$A_s=\begin{cases} c^{-3}-\dfrac{B}{5}, & B\geqslant 0 \\ -\dfrac{4}{3}\dfrac{B}{\exp(Bc^3)+\left(1+\dfrac{1}{2Bc^3}\right)\sqrt{-\pi Bc^3}\,\mathrm{erf}(\sqrt{-Bc^3})}, & B<0. \end{cases} \tag{2}$$

In Eqs. (1) and (2) c denotes the elongation parameter (the length of the nucleus is equal to $2c$ in units of the spherical nucleus radius R_0), the parameter h describes a variation in the thickness of the neck for a given elongation of the nucleus, and the parameter of the ''mirror'' (mass) asymmetry α' determines the ratio of the volumes (masses) of future fragments. In the symmetrical case $\alpha'=0$ a family of symmetric shapes is obtained, ranging from the spherical shape $(c=1,h=0)$ to the two-fragment shapes $(A_s<0)$. For the case of $\alpha'\neq 0$ different asymmetric shapes are obtained. A careful comparison of the Eq. (1) with the equation of the surface function in the original $\{c,h,\alpha\}$ parametrization shows that we have introduced a different mass asymmetry parameter scaled with elongation

$$\alpha'=\alpha c^3. \tag{3}$$

The advantages of using this mass asymmetry parameter in-

stead of α in the framework of the $\{c,h,\alpha\}$ parametrization were pointed out and discussed by Pauli [23] many years ago.

Within the framework of the chosen parametrization one can introduce collective coordinates that are more natural from the physical point of view. These coordinates for fission process are R [19,21] that is the distance between the centers of mass of future fragments, and η [24–26] that is equal to the ratio of the difference of the fragments mass to their sum $\eta=(A_1-A_2)/(A_1+A_2)$. The coordinates R and η have been often used [6,13–15,23–26] as the elongation and the mass asymmetry collective coordinates. It is particularly convenient to use R and η when one is investigating the energy and mass distributions of fission fragments.

The mass asymmetry parameter α' is proportional to the mass asymmetry coordinate η, as

$$\eta=\frac{3}{8}\alpha'. \tag{4}$$

Furthermore, the mass asymmetry parameter α' is simply related to the mass (volume) ratio of forming fragments

$$\frac{A_1}{A_2}=\frac{V_1}{V_2}=\frac{1+\frac{3}{8}\alpha'}{1-\frac{3}{8}\alpha'}, \tag{5}$$

which is defined as the ratio of the volumes of two parts of the nucleus obtained when the latter is intersected by the plane $z=0$ [23,27].

It is also interesting to note that R and η are the first two collective coordinates in the theoretical scheme [28] that uses the multipole moments of nuclear density for specifying the collective coordinates. However, the use of the collective coordinates (R,h,η) instead of the coordinates (c,h,α') leads in three-dimensional Langevin calculations to serious computational problems. It is evident that there are no explicit expressions for dependence of the shape parameters (c,h,α') on the coordinates (R,h,η). Therefore it is necessary to carry out tiresome recalculations that substantially increase the computational time. Because of these disadvantages and computational difficulties, we have chosen the geometrical shape parameters as the collective coordinates: $(c,h,\alpha')=(q_1,q_2,q_3)$. The most important advantage of this choice is the possibility to enlarge considerably the dimension of the grid with respect to the constriction parameter h and the elongation parameter c. This enlargement is very desirable for modeling the fission dynamics in the stochastic approach, but it is impossible in the original version of the $\{c,h,\alpha\}$ parametrization.

B. Basic equations

In the stochastic approach evolution of the collective coordinates is [1–4] considered as motion of Brownian particles that interact stochastically with a large number of internal degrees of freedom, constituting the surrounding ''heat bath.'' The hydrodynamical friction force is assumed to be derived from the random force averaged over a time larger than the collisional time scale between collective and internal degrees of freedom. The random part is modeled as a Gaussian white noise that causes fluctuations of the collective variables, and, as a final result, fluctuations of the physical observables in fission process. The coupled Langevin equations used in the dynamical calculations have the form

$$\dot{q}_i=\mu_{ij}p_j,$$

$$\dot{p}_i=-\frac{1}{2}p_jp_k\frac{\partial\mu_{jk}}{\partial q_i}-\frac{\partial V}{\partial q_i}-\gamma_{ij}\mu_{jk}p_k+\theta_{ij}\xi_j, \tag{6}$$

where $\mathbf{q}=(c,h,\alpha')$ are the collective coordinates, $\mathbf{p}=(p_c,p_h,p_{\alpha'})$ are the conjugate momenta, $V(\mathbf{q})$ is the potential energy, m_{ij} ($\|\mu_{ij}\|=\|m_{ij}\|^{-1}$) is the tensor of inertia, γ_{ij} is the friction tensor, $\theta_{ij}\xi_j$ is a random force, and ξ_j is a random variable satisfying the relations

$$\langle\xi_i\rangle=0,$$

$$\langle\xi_i(t_1)\xi_j(t_2)\rangle=2\delta_{ij}\delta(t_1-t_2). \tag{7}$$

Thus, the Marcovian approximation is assumed to be valid. In these equations, and further in this paper, we use the convention that repeated indices are to be summed over from 1 to 3, and the angular brackets denote averaging over an ensemble.

Eigenvalues and eigenvectors of the diffusion matrix D_{ij}, which are used [4] for calculation of the strength of random force, have been calculated by the Jacoby method [29]. The strengths of the random force are related to the diffusion tensor D_{ij} by the equation

$$D_{ij}=\theta_{ik}\theta_{kj}, \tag{8}$$

which, in turn, satisfies the Einstein relation

$$D_{ij}=T\gamma_{ij}. \tag{9}$$

Here T is the temperature of the ''heat bath'' which is determined by the Fermi-gas model [30] formula

$$T=[E_{int}/a(\mathbf{q})]^{1/2}, \tag{10}$$

where E_{int} is the internal excitation energy of the nucleus, and $a(\mathbf{q})$ is the level density parameter that depends on the collective coordinates as follows:

$$a(\mathbf{q})=a_vA+a_sA^{2/3}B_s(\mathbf{q}), \tag{11}$$

where A is the mass number of the compound nucleus, and B_s is the dimensionless functional of the surface energy in the LDM with a sharp surface [19,22]. The values of the parameters $a_v=0.073$ MeV^{-1}, $a_s=0.095$ MeV^{-1} in Eq. (11) have been taken from the work of Ignatyuk *et al.* [31].

During a random walk along the Langevin trajectory in space of the collective coordinates, the energy conservation law has been used in the form

$$E^*=E_{\rm int}+E_{\rm coll}+V(\mathbf{q})+E_{\rm evap}(t), \tag{12}$$

where E^* is the total excitation energy of the nucleus, $E_{\rm coll}$ is the kinetic energy of the collective degrees of freedom, and $E_{\rm evap}(t)$ is the energy carried away by evaporated particles by the time t.

The Langevin trajectories are simulated starting from the ground state with the excitation energy E^* of the compound nucleus. The initial conditions were chosen by the Neumann method with the generating function

$$P(\mathbf{q}_0,\mathbf{p}_0,l,t=0)\sim\exp\left\{-\frac{V(\mathbf{q}_0)+E_{\rm coll}(\mathbf{q}_0,\mathbf{p}_0)}{T}\right\}\times\delta(\mathbf{q}-\mathbf{q_0})F(l). \quad (13)$$

In the used approach it is necessary to choose the initial state of the fissioning system at its ground state for each partial wave l. But for large values of l a potential energy pocket disappears, and the choice of initial collective coordinates becomes undefined. Therefore, we start modeling fission dynamics from a spherical nucleus, i.e., $\mathbf{q_0}=(c_0=1.0,h_0=0.0,\alpha_0'=0.0)$. The initial state is assumed to be characterized by the thermal equilibrium momentum distribution, and by a spin distribution $F(l)$ for heavy-ion complete fusion. This choice of the initial conditions means that we restrict ourselves to a situation where an equilibrated compound nucleus has been formed in a heavy-ion fusion reaction before the fission process starts. Therefore, the formalism of the present model is not suitable to describe quasifission (fast fission) reactions. Contrary to the calculations [13,14,16] performed for zero angular momentum, the spin distribution has been taken into account in these calculations. We have parametrized the compound nuclei spin distribution $F(l)$ according to the scaled prescription [4,10], which reproduces to a certain extent the dynamical results of the surface friction model [32] for fusion of two heavy ions. At the end of the discussion concerning the initial conditions given by Eq. (13) it should also be noted that for fusion-fission reactions at high excitation energies, and especially at a high angular momentum, the traditional concept of an equilibrated compound nucleus with fixed excitation energy appears to be a rather unrealistic idealization of the real complicated situation.

The potential energy of the nucleus was calculated within the framework of a macroscopic model with finite range of the nuclear forces [33,34]. The potential energy was obtained as a sum of the Coulomb energy, the generalized surface energy (the nuclear interaction energy), and the rotational energy, as usual. The parameters of the model were taken from Ref. [34]. In contrast to Refs. [6,18], where the potential energy was calculated in the harmonic approximation: $V(c,h,\alpha)=V(c,h,\alpha=0)+C_\alpha^2/2$, using the local stiffness C_α with respect to the mass asymmetry coordinate α, similar assumptions have not been done in the present work. The potential energy, as well as the other transport coefficients of the Langevin equations, have been calculated on the uniform three-dimensional grid with $151\times101\times51$ grid points and $c\in[0.7,3.7]$, $h\in[-0.6,0.4]$, and $\alpha'\in[-1,1]$. Interpolation between the grid points has been performed using the Lagrange formulas.

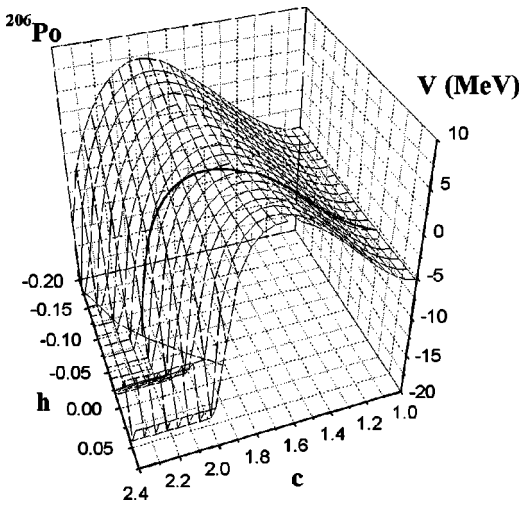

FIG. 1. The potential energy surface for the compound nucleus ^{206}Po in the case of $\alpha'=0$ at zero angular momentum. The thick solid curve is the mean dynamical trajectory. The thin line is the scission line determined from the intersection of the scission surface (see text for explanation) and the plane $\alpha'=0$. The mean dynamical trajectory was calculated with the reduction coefficient $k_s=0.25$.

It is well known [30,35] that in order to calculate the conservative part of the driving forces governing the collective motion of the thermodynamical system one should use a thermodynamical potential (for instance the free energy [2] or the entropy [4]) rather than the bare potential. Unfortunately, there is a large uncertainty in the temperature-dependent parameters of the LDM with a sharp surface [36–38]. Just recently [39] the finite-range LDM with a Yukawa-plus-exponential nucleon-nucleon interaction has been generalized to describe the temperature dependence of the free energy. Therefore, it is more reliable and reasonable, in our opinion, to use for the first three-dimensional Langevin calculations, presented in this paper, the potential energy instead of the free energy. Possible improvements in this direction could be made in future studies.

The potential energy surfaces for the nuclei ^{206}Po and ^{260}Rf in the coordinates c and h are shown in Figs. 1 and 2, with the mean dynamical trajectories of the fissioning system during its evolution from the ground state to scission. The mean dynamical trajectory is a trajectory obtained in our dynamical Langevin calculations by averaging over a trajectory ensemble. In this case the Langevin equations coincide with the generalized Hamilton equations, since the term responsible for fluctuations (the random force) drops out after averaging. The initial conditions were chosen at the saddle point, with $\alpha'=0$ and $p_{\alpha'}=0$. For ^{260}Rf the saddle point coincides practically with the ground state. While the system evolves from the saddle point to scission, the averaged values of the mass asymmetry parameter and the conjugate momentum are identically equal to zero, due to the initial conditions. So the mean dynamical trajectories lie in the (c,h) plane and are identical to those obtained from the solution of the generalized Hamilton equations [40]. Figure 3 shows some selected shapes resulting from Eqs. (1) and (2) for a

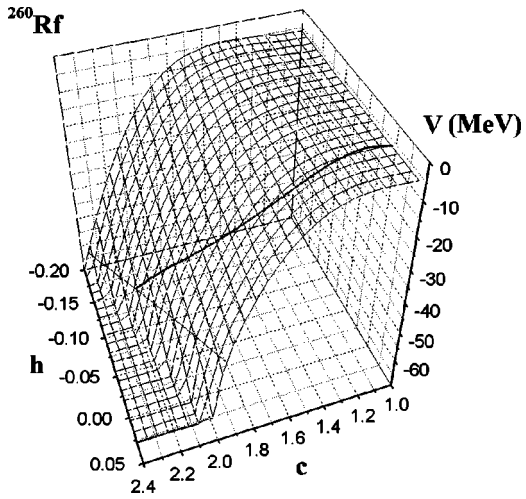

FIG. 2. The same as in Fig. 1, but for the compound nucleus ^{260}Rf. The mean dynamical trajectory was calculated with the reduction coefficient $k_s=0.25$.

few values c and h, as well as an illustrative sequence of shapes along the mean dynamical trajectory from the ground state of the fissioning nucleus through the saddle point to its scission. As was noted above, the main distinction of this figure from the analogous figures in Refs. [19,20] is the considerably enlarged dimension of the grid with respect to the constriction parameter h and the elongation parameter c. It is desirable for modeling of random walk of Brownian particles in the collective coordinate space.

Intersection of a mean dynamical trajectory with a scission surface determines the mean scission point. In our calculations made with the potential energy surfaces shown in Figs. 1 and 2, and the reduction coefficient $k_s=0.25$, this point has the following values of coordinates: $c_{sc}=2.1$, $h_{sc}=-0.07$ for the nucleus ^{206}Po and $c_{sc}=2.2$, $h_{sc}=-0.11$ for the nucleus ^{260}Rf. It is in a good agreement with our previous calculations in the diffusion model [6]. The values of the repulsive Coulomb and the nuclear attractive energies together with the prescission kinetic energy determine the value of the total kinetic energy of fission fragments. Fluctuations of the scission points of the individual stochastic Langevin trajectories around the mean scission point determine the value of the variance of the fission fragment mass and kinetic-energy distributions (see a more detailed quantitative discussion in Sec. III).

The inertia tensor is calculated by means of the Werner-Wheeler approximation for incompressible irrotational flow. Description of the method is given, for example, in Ref. [40]. It was shown in Ref. [41] that the Werner-Wheeler method allows, with surprisingly high accuracy, to perfom calculation of the inertia tensor for almost all shapes of the fissioning nucleus, with the exception of the zero neck radius configurations.

A modified one-body mechanism of nuclear dissipation [42,43] has been used for determination of the dissipative part of the driving forces. The expression applied to calculate the friction tensor for so-called surface-plus-window dissipation reads as follows:

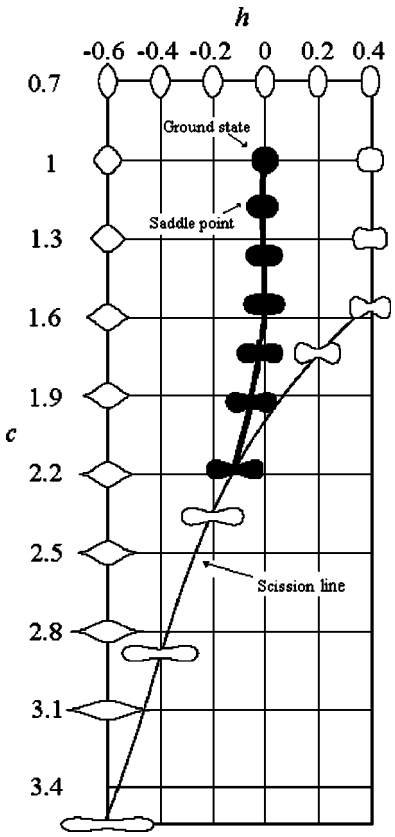

FIG. 3. Illustration of the parametrization of the nuclear shapes obtained from Eq. (1). The asymmetry parameter α' is fixed to zero to yield shapes with reflection symmetry about the plane $z=0$. The thick solid curve indicates the mean dynamical trajectory for the compound nucleus ^{260}Rf from the saddle point to the ground state and from the saddle point to the scission point. The reduction coefficient $k_s=0.25$.

$$\gamma_{ij}=\frac{1}{2}\rho_m\bar{v}\left\{\frac{\partial R}{\partial q_i}\frac{\partial R}{\partial q_j}\Delta\sigma+\frac{32}{9}\frac{1}{\Delta\sigma}\frac{\partial V_1}{\partial q_i}\frac{\partial V_1}{\partial q_j}\right.$$
$$+k_s\pi\left[\int_{z_{\min}}^{z_N}\left(\frac{\partial\rho_s^2}{\partial q_i}+\frac{\partial\rho_s^2}{\partial z}\frac{\partial D_1}{\partial q_i}\right)\left(\frac{\partial\rho_s^2}{\partial q_j}+\frac{\partial\rho_s^2}{\partial z}\frac{\partial D_1}{\partial q_j}\right)\right.$$
$$\times\left(\rho_s^2+\left(\frac{1}{2}\frac{\partial\rho_s^2}{\partial z}\right)^2\right)^{-1/2}dz+\int_{z_N}^{z_{\max}}\left(\frac{\partial\rho_s^2}{\partial q_i}+\frac{\partial\rho_s^2}{\partial z}\frac{\partial D_2}{\partial q_i}\right)$$
$$\left.\left.\times\left(\frac{\partial\rho_s^2}{\partial q_j}+\frac{\partial\rho_s^2}{\partial z}\frac{\partial D_2}{\partial q_j}\right)\left(\rho_s^2+\left(\frac{1}{2}\frac{\partial\rho_s^2}{\partial z}\right)^2\right)^{-1/2}dz\right]\right\},\quad(14)$$

where ρ_m is the mass density of the nucleus, $\bar{v}$ is the average nucleon speed inside the nucleus, $\Delta\sigma$ is the area of window between two parts of the system, D_1, D_2 are the positions of mass centers of two parts of the fissioning system relative to the center of mass of the whole system, z_{min} and z_{max} are the left and right ends of the nuclear shape, z_N is the position of the neck plane that divides the nucleus into two parts. We have chosen the position of the z_N at minimum of $\rho_s^2(z)$, but not at the $z_N=0$, as it was assumed in Refs. [23,27]. This formula is reduced for the symmetrical forms and be-

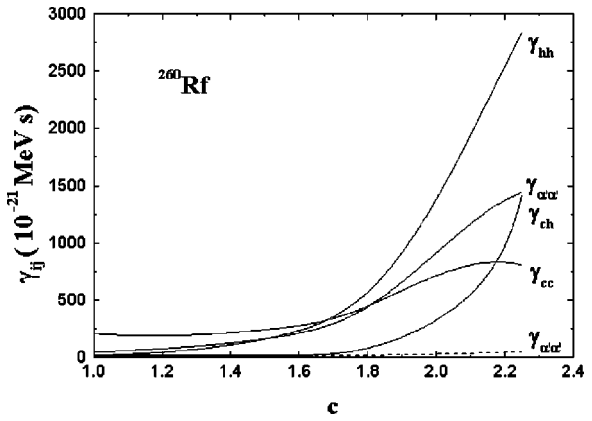

FIG. 4. The components of the friction tensor along the mean dynamical trajectory for the compound nucleus ^{260}Rf as the functions of the elongation parameter c. The dashed curve is the $\gamma_{\alpha'\alpha'}$ component without additional term in Eq. (14). The components $\gamma_{c\alpha'}$ and $\gamma_{h\alpha'}$ are equal to zero in the case where $\alpha'=0$. The reduction coefficient $k_s=0.25$.

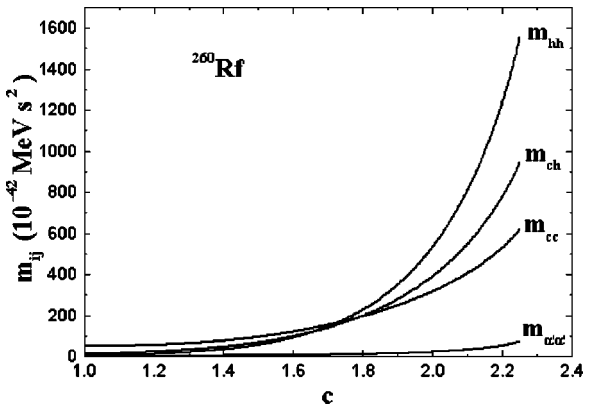

FIG. 5. The components of the inertia tensor along the mean dynamical trajectory for the compound nuclei ^{260}Rf as the functions of the elongation parameter c. The components $m_{c\alpha'}$ and $m_{h\alpha'}$ are equal to zero in the case where $\alpha'=0$.

comes similar to the one presented in Ref. [44]; k_s is the reduction coefficient of the contribution from the wall formula in Refs. [44,45]. The value $k_s=1$ corresponds to the classic wall-and-window dissipation formula [45]. A quantum treatment of one-body dissipation showed [46] that the nuclear viscosity is only about 10% of the value calculated in accordance with the wall expression, although the functional dependence of the one-body dissipation on a change in the nuclear shape is correctly reproduced by the wall expression. Therefore, in the modified variant of one-body dissipation, proposed in Refs. [42,43], which is called the surface-plus-window dissipation, the contribution to the dissipation due to collisions of nucleons with the nuclear surface was appreciably reduced (by almost four times; the reduction coefficient $k_s=0.27$). This value of k_s was obtained [42] from analyzing experimental data on the widths of giant resonances. However, comparison of the calculated results with the experimental data of the mean values of the total kinetic energy of fission fragments for all fissioning nuclei throughout the periodic system suggests [43] the limits $0.2\leqslant k_s\leqslant 0.5$. Elucidation of the mechanism of nuclear viscosity in fission and a reliable estimation of its value continue to be essentially open questions.

In Eq. (14) the original wall-and-window formula [45] was completed by an additional term, following [5,47] [the second term in bold curly braces in Eq. (14)], which takes into account the dissipation associated with the relative changes of two interacting nascent fragments. From Fig. 4 one can see that this term gives an appreciable contribution to the diagonal mass asymmetry component of the friction tensor $\gamma_{\alpha'\alpha'}$ and, hence, to the corresponding component of the diffusion tensor $D_{\alpha'\alpha'}$. And, as a final result, this term strongly influences the values of the variance of the fission fragment mass distribution. Dynamical calculations without this term would be strongly inadequate, as it is mentioned in [47]. Our two-dimensional calculations [16] of the fission fragment mass distribution agree with this statement.

For strongly necked-in shapes the friction tensor has been calculated using the wall-and-window formula, Eq. (14). For compact mononuclear shapes only the wall formula has been used with the reduction factor k_s. In the intermediate case for the shapes that are neither compact nor strongly necked-in a smooth interpolation [48] between the wall and the wall-and-window formulas has been used, with a form factor going to 1 for mononuclearlike shapes, and going to 0 for the shapes with zero neck radius.

Figures 4 and 5 show the components of the friction and the inertia tensors as functions of the elongation parameter c from the ground state of the fissioning system to its scission along the mean dynamical trajectory. It can be seen that all components of the both tensors have smooth behavior. It should be noted that the both friction tensor and the inertia tensor are essentially nondiagonal over a great part of evolution of the fissioning system from the ground state to scission. This is the reason for an appreciable deviation of the mean dynamical trajectory from the bottom of the fission valley (see Figs. 2 and 3). The diagonal components increase, especially m_{hh} and γ_{hh}, while the fissioning system approaches to scission. The main features of the dependences of m_{ij} and γ_{ij} are rather similar to those described earlier in Refs. [6,14]. Figures 2 and 3 draw attention to the fact that from the very beginning of descent from the saddle point the mean dynamical trajectory deviates appreciably from the bottom of the fission valley (line $h=0$ fits approximately the bottom of the fission valley). The reason for this is obviously the strong nondiagonality of the inertia and friction tensors in the (c,h) coordinates (see Figs. 4 and 5). The calculated components of the inertia tensor show that these coordinates are not normal coordinates, and the c and h modes cannot be considered as independent. This is indicated by the value of the nondiagonal component of the inertia tensor m_{ch} being, on the average, of the same order of magnitude as the product of the diagonal components of the inertia tensor m_{cc} and m_{hh}, i.e., $m_{ch}^2/(m_{cc}m_{hh})\approx 1$. In an ideal parametrization in which the collective coordinates are normal (or almost normal) this ratio should be small, and the mean dynamical trajectory should pass near the bottom of the fission valley. It was pointed out in Ref. [19] that the coordinates (R,h) are

more natural dynamical coordinates and can be regarded as approximately independent. As the calculations showed, the nondiagonality of the tensors m_{ij} and γ_{ij} is expressed much less strongly in the coordinates (R,h) than in the coordinates (c,h), and therefore the mean dynamical trajectories should pass closer to the corresponding bottom of the fission valley.

Study of deep-inelastic collisions gives much information on nuclear dissipation. These are grazing collisions where the dinuclear systems are connected by a relatively thin neck. There is a little mass transfer on the average, and interpretation of the data, although indicating high dissipation, is ambiguous. Study of dissipation in fusion-fission and quasifission reactions is of great interest because it might [36] shed light on dissipation in the mononuclear systems, perhaps, it might give information on the effects of symmetries [49], and on the role of chaos [50], particularly at the stage of the process before the saddle point is reached.

Evaporation of the prescission light particles is incorporated in the present model as follows. During the temporal evolution of the fission trajectory the internal excitation energy is calculated at each time step. Correspondingly, the partial evaporation widths Γ_j $(j=n,p,d,t,^3\mathrm{He},\alpha,\gamma)$, the total width $\Gamma_{\mathrm{tot}}=\Sigma_j\Gamma_j$, and the mean evaporation time $\tau_{\mathrm{tot}}=\hbar/\Gamma_{\mathrm{tot}}$ are calculated by the Weisskopf formula [51,52]. The Langevin equations are integrated by means of the Heuen finite difference scheme [4,12] of the first order. The step of integration is Δt. Knowing the time step of the difference scheme we can determine the probability for the nucleus to evaporate a particle using the following procedure [53,54]: a random number ζ uniformly distributed in the interval $(0,1)$ is generated and compared with the ratio of the time step Δt to the mean evaporation time τ_{tot}. It is assumed that one of the particles $(n,p,d,t,^3\mathrm{He},\alpha,\gamma)$ is evaporated if $\zeta<\Delta t/\tau_{\mathrm{tot}}$. A specific particle is chosen by means of Monte Carlo sampling, the probability of emitting a given particle is proportional to the relevant partial width Γ_j. This procedure allows one to treat particle evaporation discretely, and not in the continuous approximation [11,12], and simulates the law of radioactive decay with half-life τ_{tot}. Among the prescission light particles neutrons play a special role [55], because their number is much greater than the number of evaporated charged particles ($p,d,t,^3$He, and α particles) or γ quanta. The mean multiplicity of the prescission neutrons is a measure of the time scale of the fission process. It is a kind of nuclear clock [55,56] that enables one to evaluate the time spent by the fissioning nucleus between its ground state and scission configurations. A direct confrontation of the experimental data on prescission neutron multiplicities with the calculated results in the framework of the stochastic approach based on the Langevin or the Fokker-Planck equations has allowed [3,12] a qualitative determination of the key parameter, entering this description, namely the nuclear friction. Therefore, one of the main goals of the present calculations is to determine the value of the reduction factor k_s of surface-plus-window dissipation by comparing the experimental data on the MED of fission fragments and the prescission neutron multiplicities with our calculated results.

III. RESULTS AND DISCUSSIONS

A. Discussion of calculated results of the fission fragment MED

We have carried out calculations of the observables in fission of the compound nuclei ^{206}Po, ^{224}Th, ^{244}Cm, and ^{260}Rf formed in the following heavy-ion reactions:

$$(1)\ {}^{12}\mathrm{C}+{}^{194}\mathrm{Pt}\rightarrow{}^{206}\mathrm{Po}\quad (E_{lab}=99\ \mathrm{MeV});$$

$$(2)\ {}^{16}\mathrm{O}+{}^{208}\mathrm{Pb}\rightarrow{}^{224}\mathrm{Th}\quad (E_{lab}=108\ \mathrm{MeV});$$

$$(3)\ {}^{12}\mathrm{C}+{}^{232}Th\rightarrow{}^{244}\mathrm{Cm}\quad (E_{lab}=97\ \mathrm{MeV});$$

$$(4)\ {}^{20}\mathrm{Ne}+{}^{240}\mathrm{Pu}\rightarrow{}^{260}\mathrm{Rf}\quad (E_{lab}=142\ \text{and}\ 174\ \mathrm{MeV}).$$

Our calculated results and the experimental data from Refs. [57–60] are summarized in Tables I and II.

The fullest and clearest representation of the calculations of the fission fragment MED is in the form of contour diagrams of the distribution $Y(E_K,M)$. The typical diagrams calculated in the stochastic approach based on the three-dimensional Langevin equations are shown in Figs. 6 and 7, for example, for the compound nucleus ^{260}Rf for two excitation energies. For comparison, Figs. 6 and 7 also show the experimental diagrams taken from Ref. [57]. We first must note a good agreement in the general behavior of the contours in the experimental and theoretical diagrams. The contour diagrams calculated in the present study are completely similar to those obtained in Ref. [17] in the framework of the dynamical model with zero viscosity, although the method of calculating $Y(E_K,M)$ in Ref. [17] and that applied in the present work were different. It can be seen from Figs. 6 and 7 that near the maximum of $Y(E_K,M)$ the shapes of the contours are nearly ellipsoidal, whereas in the region of small $Y(E_K,M)$ the contours become similar to triangles with rounded corners. The same change in the shape of the contours was noted in Refs. [17,18]. In Figs. 6 and 7 one can see how with increasing of the excitation energy the width of the fission fragment MED increases (for a quantitative analysis of this increasing of the variance of the fission fragment mass distribution σ_M^2 and the fission fragment kinetic-energy distribution $\sigma_{E_K}^2$ see the next section and Table II). The contour diagrams also clearly show the existing liquid-drop correlation of the ratio of masses and kinetic energies of fission fragments. One of characteristic manifestations of this correlation is the presence, at fixed M, of maxima in the distributions $Y(E_K,M)$ in the region of small E_K. No doubt, such a shape of these local distributions does not indicate an asymmetric fission, the existence of which would be reflected quite differently in the shape of the $Y(E_K,M)$ contours (see, for example, Ref. [61]).

Using the calculated distribution $Y(E_K,M)$ we can find all the parameters that characterize it, and in terms of which the experimental data are usually discussed and compared with the predictions of theoretical approaches. These are, first and foremost, the first and second moments of the one-dimensional mass and energy distributions, which are ob-

TABLE I. Calculated results for the fission of ^{206}Po, ^{224}Th, and ^{244}Cm formed in the reactions $^{12}C+^{194}Pt\rightarrow{}^{206}Po$ ($E_{lab}=99$ MeV); $^{16}O+^{208}Pb\rightarrow{}^{224}Th$ ($E_{lab}=108$ MeV); $^{12}C+^{232}Th\rightarrow{}^{244}Cm$ ($E_{lab}=97$ MeV). The columns contain (from left to right) the compound nucleus (CN), the excitation energy (E^*), the reduction coefficient of surface-plus-window dissipation k_s, the variance of the mass and kinetic-energy distributions of fission fragments (σ_M^2 and $\sigma_{E_K}^2$), the average total kinetic energy ($\langle E_K\rangle$), the mean prescission neutron multiplicity ($\langle n_{pre}\rangle$), the average time of collective motion of the compound nucleus from its formation to the scission configurations ($\langle t_f\rangle$), and the average temperature of the compound nucleus at its scission ($\langle T_{sc}\rangle$).

CN	E^* (MeV)	k_s	σ_M^2 (u^2)	$\sigma_{E_K}^2$ (MeV^2)	$\langle E_K\rangle$ (MeV)	$\langle n_{pre}\rangle$	$\langle t_f\rangle$ (10^{-21} s)	$\langle T_{sc}\rangle$ (MeV)
^{206}Po	76.6							
		0.10	341±31	375±34	144.9±0.6	1.5	26	1.97
		0.25	280±26	180±17	144.5±0.4	2.8	111	1.82
		0.50	234±24	121±12	143.0±0.4	3.6	213	1.73
		1.00	222±25	114±13	131.0±0.4	3.9	305	1.69
Expt. [57]			165±4	106±3	146.5±0.8	2.8		
^{224}Th	53.8							
		0.10	322±21	158±10	154.7±0.3	0.7	22	1.75
		0.25	272±17	121±8	154.3±0.2	1.5	65	1.67
		0.50	243±13	105±6	154.1±0.2	2.2	141	1.59
		1.00	203±21	96±9	154.0±0.4	2.7	258	1.53
Expt. [59,60] [a]			213	137	162.4±1.	2.5		
^{244}Cm	69.2							
		0.10	364±19	210±11	172.6±0.3	1.4	13	1.92
		0.25	315±14	155±7	172.4±0.2	2.0	24	1.88
		0.50	271±23	132±11	172.1±0.3	3.2	64	1.76
		1.00	233±35	120±18	172.0±0.5	4.2	154	1.65
Expt. [58]			366	259	178	3.0		

[a]The experimental values of $\langle n_{pre}\rangle$ have been taken from [59]. Experimental values of the variance and the mean kinetic energies have been taken from [60] for ^{224}Th compound nucleus.

tained by integrating $Y(E_K,M)$ over E_K and M, respectively. Of interest then are the functions $\langle E_K(M)\rangle$, $\sigma_{E_K}^2(M)$, and $\sigma_M^2(E_K)$ (the mean value of the fragment kinetic energy and its variance at a fixed value of M and the variance of fission fragment mass distribution at a fixed value of E_K), which reflect correlation of the parameters of the fission fragment MED. All information about the characteristics of the MED of fission fragments will be discussed later on in terms of the one-dimensional mass and energy distributions, which are obtained from the fission fragment MED by integrating it

TABLE II. The same as in Table I, but for the fission of ^{260}Rf formed in the reactions $^{20}Ne+^{240}Pu\rightarrow{}^{260}Rf$ ($E_{lab}=142$ and 174 MeV).

CN	E^* (MeV)	k_s	σ_M^2 (u^2)	$\sigma_{E_K}^2$ (MeV^2)	$\langle E_K\rangle$ (MeV)	$\langle n_{pre}\rangle$	$\langle t_f\rangle$ (10^{-21} s)	$\langle T_{sc}\rangle$ (MeV)
^{260}Rf	74.2							
		0.10	417±7	362±6	199.5±0.1	0.7	7	2.13
		0.25	365±12	217±7	201.1±0.2	1.3	15	2.11
		0.50	315±14	187±8	201.0±0.2	2.0	30	2.06
		1.00	254±25	173±17	200.3±0.5	2.9	69	1.98
Expt. [57]			506±12	372±13	195±2	3.5		
^{260}Rf	103.8							
		0.10	506±10	581±12	197.1±0.2	1.1	6	2.33
		0.25	404±15	280±10	201.3±0.2	2.0	12	2.29
		0.50	325±13	215±6	200.3±0.2	3.1	26	2.21
		1.00	281±13	201±10	195.8±0.2	4.3	60	2.1
Expt. [57]			620±17	424±15	196±2	5.7		

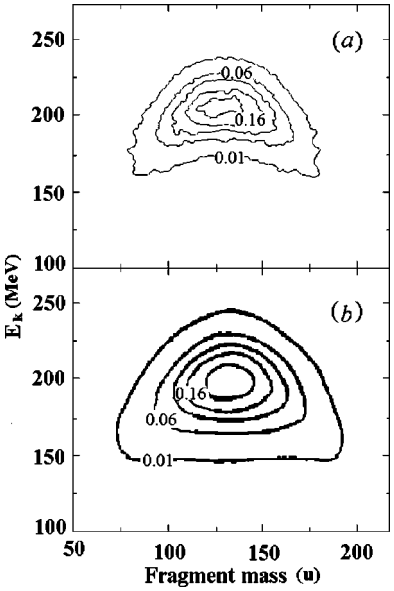

FIG. 6. The theoretical (a) and experimental (b) MED of fission fragments of ^{260}Rf at the total excitation energy $E^*=74.2$ MeV. The numbers at the contour lines in percents indicate the yield, which is normalized to 200%. The theoretical diagram was calculated with the reduction coefficient $k_s=0.1$. The experimental diagram was taken from Ref. [57].

over kinetic energy or mass, respectively. We shall also consider the correlation of the $Y(E_K,M)$ parameters.

B. First and second moments of the fission fragment energy and mass distributions

The energy distribution $Y(E_K)$ has the form of a curve with one maximum and is usually approximated in both the experimental and the theoretical studies by a Gaussian function characterized by the mean value $\langle E_K\rangle$ and the variance $\sigma^2_{E_K}$. Similarly, the mass distribution $Y(M)$ is also approximated at a sufficiently high excitation energy by the Gaussian function with the mean value $\langle M\rangle$ and the variance σ^2_M. Approximation of these one-dimensional distributions by the Gaussian functions is convenient and standard, but its accuracy may often be unsatisfactory [62].

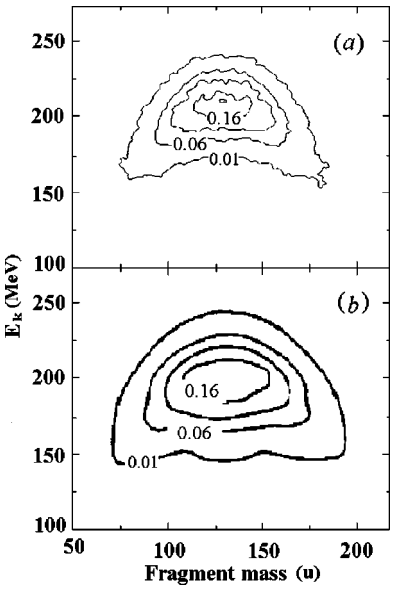

FIG. 7. The same as in Fig. 6, but for $E^*=103.8$ MeV.

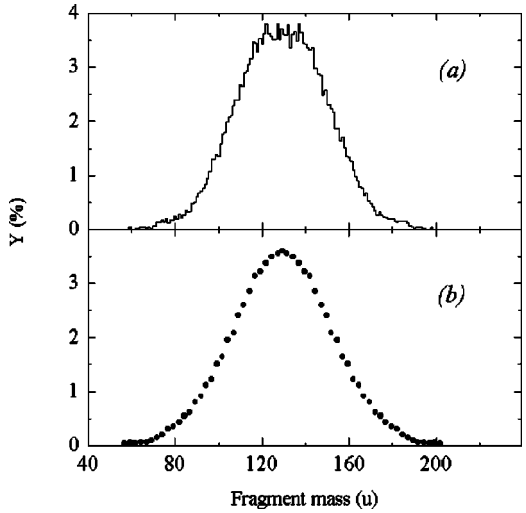

FIG. 8. The theoretical (a) and experimental (b) mass distributions of fission fragments of ^{260}Rf, $E^*=74.2$ MeV. The theoretical histogram was calculated with the reduction coefficient $k_s=0.1$. The experimental distribution was taken from Ref. [57].

Figures 8 and 9 show the mass and energy distributions for the compound nucleus ^{260}Rf. For comparison, Fig. 8 also shows the experimental mass distribution taken from Ref. [57]. Unfortunately, the figure showing the experimental energy distribution of fission fragments is not presented in Ref. [57], and we could not compare directly the calculated and the experimental distributions, in contrast to the case of the mass distribution. One can see that the calculated kinetic-energy distribution of fission fragments shown in Fig. 9 noticeably differs from the Gaussian distribution. The extent of the deviation of these distributions from the Gaussian distributions can be expressed in terms of asymmetry coefficient and excess [6,13,17,62], i.e., quantities associated with the third and fourth moments of the distributions. The calculated excess of the energy distribution indicates that it has a

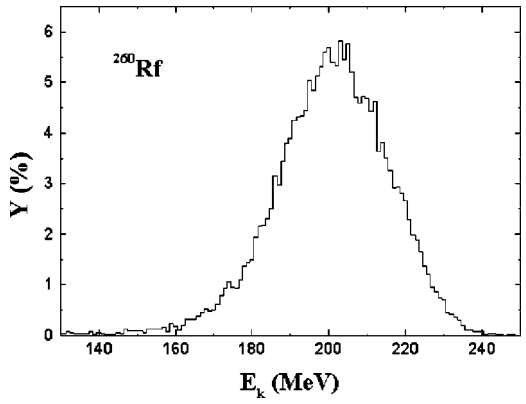

FIG. 9. The calculated energy distribution of fission fragments of ^{260}Rf, $E^*=74.2$ MeV. The reduction coefficient $k_s=0.1$.

sharper peak than the Gaussian function (the excess is about one). Furthermore, there is no symmetry of the energy distribution with respect to $\langle E_K \rangle$—the asymmetry coefficient is significantly nonzero and negative. In comparison with the energy distribution the mass distribution of fission fragments (shown in Fig. 8) has a more Gaussian-like form (the asymmetry coefficient and the excess are almost zero).

The first and the second moments of the fission fragment kinetic-energy distribution are sensitive to the nature of descent of the fissioning nucleus from the saddle point to scission, and to the shape of scission configurations. Therefore, the experimental values of the mean fragment kinetic energy $\langle E_K \rangle$ are traditionally used as one of the most important sources of data from which estimates of the nuclear viscosity are made [40,44,62,63].

It was assumed in calculations of the parameters of the energy distribution that the total kinetic energy E_K of fission fragments is the sum of the Coulomb repulsion energy V_c, the nuclear attractive energy V_n of the nascent fragments, and the kinetic energy of their relative motion (prescission kinetic energy E_{ps}). All parts of this sum are calculated at the moment of scission. Then the mean value of the total kinetic energy $\langle E_K \rangle$ is found as

$$\langle E_K \rangle = \langle V_c \rangle + \langle V_n \rangle + \langle E_{ps} \rangle, \tag{15}$$

and the expression for its variance is

$$\sigma^2_{E_K} = \sigma^2_{\tilde{V}_c} + \sigma^2_{E_{ps}} + 2\sigma_{\tilde{V}_c E_{ps}}, \tag{16}$$

where

$$\sigma^2_{\tilde{V}_c} = \langle \tilde{V}_c^2 \rangle - \langle \tilde{V}_c \rangle^2,$$

$$\sigma^2_{E_{ps}} = \langle E_{ps}^2 \rangle - \langle E_{ps} \rangle^2, \tag{17}$$

$$\sigma_{\tilde{V}_c E_{ps}} = \langle \tilde{V}_c E_{ps} \rangle - \langle \tilde{V}_c \rangle \langle E_{ps} \rangle,$$

where

$$\tilde{V}_c = V_c + V_n .$$

The last equation means that a part of the Coulomb repulsion energy is used to overcome nuclear attraction between the nascent fragments. A simple estimation of this quantity as the surface energy of two sides of the neck has been done in Refs. [14,64]. We have exactly calculated V_n in the finite-range LDM by performing numerical evaluation of the corresponding integrals [65].

The scission configuration is determined by the intersection points of the stochastic Langevin trajectories of the fissioning system, with the scission surface in the coordinate subspace. When making three-dimensional Langevin calculations of the MED of fission fragments, especially of the fission fragment kinetic-energy distribution, the crucial problem is how to define the scission surface. For an arbitrary dimensional model it is a well-known problem of choice of the scission criterion that determines the set of configurations ensuring scission of the nucleus into fragments.

In fact, at the present time there is no unambiguous criterion of the scission condition. The condition of zero neck radius can be considered as one (the simplest) of the scission conditions. Such a definition of the scission condition is obviously unsatisfactory, since description of the nucleus in the liquid-drop model becomes meaningless when the neck radius becomes comparable with the distance between nucleons. Therefore, it has been often supposed [19,21,66] that the scission occurs at the critical deformation with a relatively thick neck. From the physical point of view it is attractive to determine the scission surface as the locus of points at which the following equation is satisfied:

$$\left(\frac{\partial^2 V}{\partial h^2} \right)_{c = \text{const},\ \alpha' = \text{const}} = 0. \tag{18}$$

This means that stability against variations in the neck thickness is lost. Such a criterion of scission can be called the criterion of instability of the nucleus with respect to variations in the thickness of its neck [6,13,19]. It should be noted that this scission condition corresponds to the shapes of the fissioning nucleus with a finite neck radius, with $0.3R_0$ on the average [14,19,21]. Another acceptable and physically sensible criterion is based on the equality of the Coulomb repulsion and the nuclear attraction forces between future fragments. It was shown in Ref. [63] that this scission condition leads to scission configurations for the actinide nuclei with approximately the same neck radius equaling $0.3R_0$. For these reasons we have chosen the scission surface as locus of points where configurations of the fissioning nucleus are the shapes with a finite neck radius of $0.3R_0$. We recognize that this intricate problem of the fission physics needs further detailed investigation in the framework of the finite-range LDM [33,34].

Comparing the mean fragment kinetic energy $\langle E_K \rangle$ calculated in the two-dimensional Langevin dynamics [11–14] for $M = A/2$ with the values of the quantity found on the basis of the two-dimensional MED of fission fragments, we must note that for light fissioning nuclei the value of $\langle E_K \rangle$ obtained by integrating the MED of fission fragments over M is less than the $\langle E_K \rangle$ for $M = A/2$ by 2–3 MeV. For heavy fissioning nuclei this difference increases up to 6–7 MeV. To make a careful comparison with the experimental data, a calculation of $\langle E_K \rangle$ in the framework of the stochastic approach must be made using the three-dimensional Langevin equations. Our calculated results for $\langle E_K \rangle$ are in a fairly good agreement with the experimental data, as well as with the fission systematics given by Ref. [62], which is more appropriate in the region $Z^2/A^{1/3} > 900$ than one given by Viola [67].

As regards the calculated values of the variance of the fission fragment kinetic-energy distribution $\sigma^2_{E_K}$ it should be stressed that the inclusion of the third collective coordinate (the mass asymmetry coordinate) leads to a considerable increase (up to 40%) of this quantity, in comparison with the two-dimensional Langevin calculations [11–14] of the fission fragment energy distribution. Qualitative estimations of the influence the mass asymmetry collective coordinate ex-

erts on the parameters of the energy distribution presented in Ref. [3] are in a good agreement with our numerical results. The results listed in tables also show that the observed appreciable growth of $\sigma^2_{E_K}$ is sufficiently well reproduced in the three-dimensional Langevin dynamics, as the compound nucleus becomes heavier. The dynamical model [17] with zero viscosity that does not take into account fluctuations of the collective variables during the temporal evolution of the fissioning nucleus from the ground state to its scission, fails completely, even in the case of qualitative description of the dependence $\sigma^2_{E_K}(Z^2/A)$.

Let us proceed to discuss the results of the computation of the variance of the fission fragment mass distribution obtained by integrating the fission fragment MED over E_K. It is clear that the mean value of the mass fragment $\langle M \rangle$ equals to $A/2$ without taking into account evaporation of the light prescission particles. Incorporation of the evaporation of the light prescission particles into the model shifts slightly the value of $\langle M \rangle$ with respect to $A/2$. As can be seen from tables, the stochastic approach based on the three-dimensional Langevin equations leads to a good agreement between the calculated and the experimental $\sigma^2_M(Z^2/A)$ values, including the region $Z^2/A > 35$. At such values of the fissility parameter the dynamical model with zero viscosity [17] and the Fong's statistical model [68] fail, as in the case of description of the dependence $\sigma^2_{E_K}(Z^2/A)$. The steep rise of the calculated dependence $\sigma^2_M(Z^2/A)$ as the fissility parameter Z^2/A increases is the result of two opposite tendencies. On one hand, during evolution of the fissioning system from the ground state to scission the stiffness $C_{\alpha'}$ grows monotonically, and fluctuations of the mass asymmetry coordinate, accordingly, fall down. But, on the other hand, when reaching the scission configuration the system still keeps in ''memory'' the former larger fluctuations. Moreover, the faster the descent of the nucleus from the saddle to scission is, the larger the remembered values of the variance of the mass asymmetry will be. Consequently, in fission of the heavier nuclei with a longer descent a larger part of the trajectory is remembered, and the variance grows rapidly. Such an interpretation of the ''memory'' of the fissioning system of its prehistory was discussed in detail at a quantitative level in Ref. [6]. Therefore, the calculated values of σ^2_M will strongly depend on the velocity of descent from the saddle point to scission and, finally, on the magnitude of nuclear viscosity. Wada and Abe [69] have come to the same conclusions about the consequences of the dynamical evolution from the saddle to scission, especially for heavy fissioning systems. The calculated values of the variance σ^2_M in the present three-dimensional Langevin calculations are larger than the corresponding values of σ^2_M obtained in the two-dimensional Langevin calculation [16] by up to 40–50 %. This considerably improves agreement with the experimental data.

Errors of the calculated parameters of the fission fragment MED arise due to the finite number of trajectories in the Langevin calculations. These purely statistical errors are calculated according to the formulas given in Ref. [70] and are presented in Tables I and II.

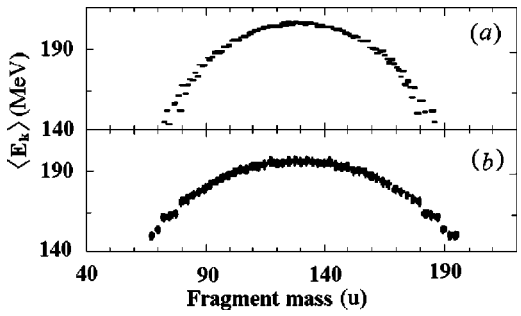

FIG. 10. The theoretical (a) and experimental (b) dependences of the mean kinetic energy $\langle E_K(M) \rangle$ on the fragment mass M for the compound nucleus ^{260}Rf at the total excitation energy $E^* = 74.2$ MeV. The reduction coefficient $k_s = 0.1$.

C. Correlation of the parameters of the fission fragment MED

Correlation of the fission fragment MED parameters carries additional information about the dynamics of descent of the fissioning system, and its very last stage, just before scission of the nucleus into fragments, in comparison with the information contained in the first and second moments of the one-dimensional mass and energy distributions. In particular, dependence of the shape of the scission configuration on the fragment mass ratio is directly reflected in correlation of the parameters of the fission fragment MED. Figures 10, 11, 12, and 13 show the dependences $\langle E_K(M) \rangle$, $\sigma^2_{E_K}(M)$, $\sigma^2_M(E_K)$ calculated in the stochastic approach, based on the three-dimensional Langevin equations. They reflect the correlation of the parameters of the fission fragment MED.

In a first approximation, the dependence $\langle E_K(M) \rangle$ can be described by the parabolic expression [71,6]

$$\langle E_K(M) \rangle = \langle E_K(A/2) \rangle \left[1 - \beta \left(1 - \frac{2M}{A} \right)^2 \right]. \qquad (19)$$

It reflects mainly dependence of the Coulomb repulsion energy and the distance between the centers of mass of future

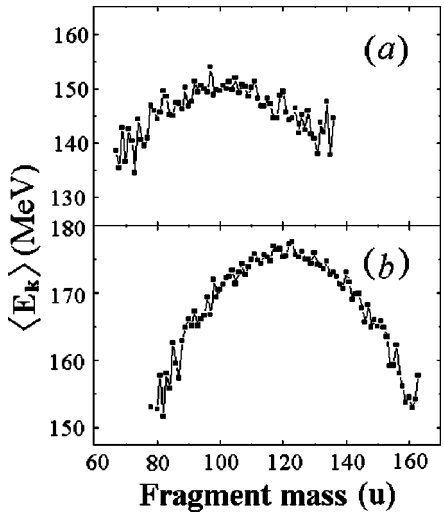

FIG. 11. The calculated dependences of the mean kinetic energy $\langle E_K(M) \rangle$ on the fragment mass M for the compound nuclei: (a) ^{206}Po and (b) ^{244}Cm. The reduction coefficient $k_s = 0.25$.

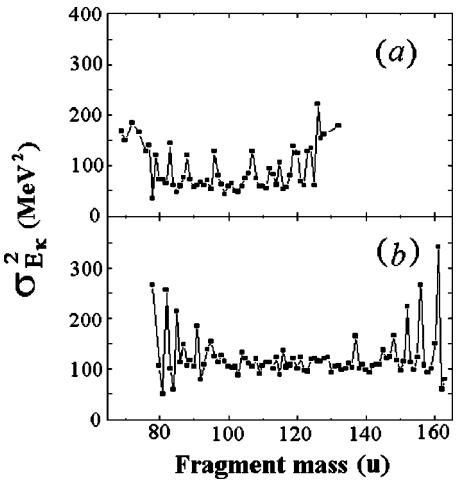

FIG. 12. The calculated dependences of the fission fragment kinetic-energy variance $\sigma^2_{E_K}$ on the fragment mass M for the compound nuclei: (a) ^{206}Po and (b) ^{244}Cm. The reduction coefficient $k_s=0.25$.

fragments at the time of scission on the fragment mass. We note that the dependence Eq. (19) for $\beta=1$ follows from the dynamical model [17] with zero viscosity. The value $\beta=1$ in Eq. (19) corresponds to the case where the kinetic energy of the fragments is determined by their Coulomb repulsion energy at the time of scission with a simplified assumption that the distance between the centers of mass of the fragments does not depend on the mass asymmetry. As was noted in Ref. [71], the experimentally observed dependence $\langle E_K(M)\rangle$ at excitation energy $E^*>20$ MeV corresponds to a value $\beta<1$ for the fissioning nuclei lighter than ^{213}At. This value depends both on the fissility parameter and on E^*. The calculated dependences $\langle E_K(M)\rangle$ correspond to the values of β that vary from $\beta=0.7$ for ^{206}Po to $\beta=1.6$ for ^{260}Rf, although they decrease faster than the experimentally observed dependences with increasing M. Allowance for the dependence of the distance between the centers of mass of the fragments at the time of scission on the mass asymmetry in the following approximations with respect to the parameter α' or $(1-2M/A)$ leads to appearance in the expression (19) of terms for $\langle E_K(M)\rangle$ that are proportional to $(1-2M/A)^4$. The analysis of $\langle E_K(M)\rangle$ made in Ref. [72] shows that the experimentally observed dependences, indeed, contain terms proportional to $(1-2M/A)^4$.

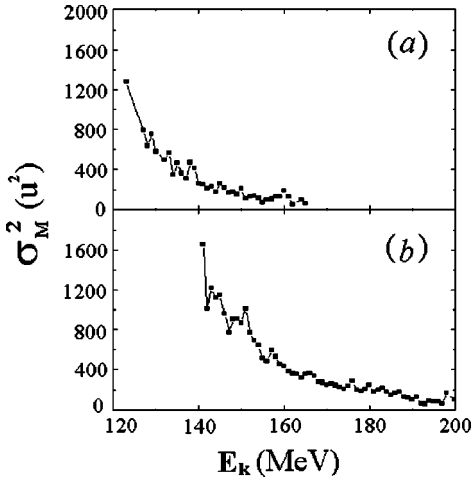

FIG. 13. The calculated dependences of the fission fragment mass variance σ^2_M on the E_K for the compound nuclei: (a) ^{206}Po and (b) ^{244}Cm. The reduction coefficient $k_s=0.25$.

The calculated variance $\sigma^2_{E_K}(M)$ is practically constant up to a certain value of the mass ratio $M/(A-M)$ that varies slightly when the parameters of the compound nucleus and the reduction factor k_s are changed. Such behavior of $\sigma^2_{E_K}(M)$ agrees well with the experimental data, whose accuracy becomes much poorer with increasing M. In accordance with the experimental data the variance $\sigma^2_M(E_K)$ of the mass distribution exhibits a characteristic decreasing dependence with increasing kinetic energy. Figure 13 shows that the theoretical description of the observed almost ''hyperbolic'' dependences $\sigma^2_M(E_K)$ is very good. Qualitatively, the dependences $\sigma^2_M(E_K)$ and $\sigma^2_{E_K}(M)$ can be understood from the form of the fission fragment MED for $M=$const and for $E_K=$const. While the former distributions have much the same width in a wide interval of M, the width and even the general form of the latter distributions strongly depend on the value of E_K.

D. The prescission neutron multiplicity, mean fission time, and deduced value of the reduction coefficient k_s

As was mentioned above, one of the ultimate objectives of these calculations is to deduce the value of the reduction coefficient of the surface-plus-window dissipation from the confrontation of the existing data on the MED of fission fragments and the prescission neutron multiplicity with the results calculated for these observables.

The results of the calculations for $k_s=0.1$, 0.25, 0.5, and 1 are listed in Tables I and II. One can see that all calculated quantities are rather sensitive to the value of the coefficient k_s. The analysis of the results presented in Tables allows us to make the following conclusions. For ^{206}Po all the observables are reproduced at the value $k_s=0.5$; for ^{224}Th and ^{244}Cm quite a good reproduction of data is achieved at $k_s=0.25$–0.5. For the heaviest compound nucleus ^{260}Rf the problem of data reproduction is more complicated. The large values of the variance $\sigma^2_{E_K}$ and σ^2_M are reproduced better in calculations at $k_s=0.1$ and $k_s=0.25$. But these values of the friction lead to a strong underestimation of the mean neutron multiplicity ($\langle n_{pre}\rangle$). Agreement between the calculated and the experimental values of $\langle n_{pre}\rangle$ becomes better at $k_s=1$ that corresponds to the full wall-and-window formula and a highly overdamped collective motion, but such a strong friction leads to considerably underestimated values of the variance of the fission fragment MED. But even at $k_s=1$ for the reaction ^{20}Ne+^{240}Pu$\rightarrow^{260}$Rf ($E_{lab}=174$ MeV) the experimental values of the prescission neutron multiplicity proved to be underestimated in the calculations. We arrived at a discrepancy in one and a half neutron (see Table II).

Thus, simultaneous description of the data on the $\langle n_{pre}\rangle$ and on the MED of fission fragments is problematic and

may even be impossible for the fissioning nuclei heavier than ^{244}Cm in the framework of the developed model. A factor that might have strong influence on the calculated values of $\langle n_{pre} \rangle$ is contribution of the evaporated neutrons during formation of the equilibrated compound nucleus, i.e., in the entrance channel of the considered reactions. The entrance channel effects have been recently discussed in Refs. [73–75]. It was shown that for some combinations of the colliding heavy ions (the reaction ^{20}Ne+^{240}Pu belongs to this case) the contribution of the evaporated neutrons during formation of the equilibrated compound nucleus can be an appreciable part of the $\langle n_{pre} \rangle$.

Tables I and II also contain the calculated values of the mean fission time $\langle t_f \rangle$. They have been calculated by averaging over a trajectory ensemble as the mean time of collective motion of the fissioning nucleus from the moment of its formation to the scission configuration. Experimentally $\langle t_f \rangle$ is rarely measured directly, but it can be deduced from the measured multiplicities of particles emitted prior to fission. Therefore, such deduced time scales of fusion-fission reactions are dependent rather strongly on the assumptions adopted in statistical model calculations of the prescission neutron multiplicities (see, as an example, Ref. [73]). The deduced values of time scales for fusion-fission reactions constitute at least several 10^{-19} s [55]. From the calculated values of $\langle t_f \rangle$ presented in tables one can see that at $k_s \geqslant 0.5$ they are of the same order of magnitude, although they decrease, with increase of the fissility parameter, faster than the experimental values [55,59].

IV. CONCLUSIONS

We have implemented three-dimensional Langevin calculations to study simultaneously the parameters of the fission fragment MED from excited compound nuclei and the mean prescission multiplicities of the light evaporated particles that dynamically compete with fission and accompany it. All these fission characteristics are rather sensitive to the magnitude of nuclear viscosity in fission process. We have chosen the shape parameters of the well-known ''funny hills'' parametrization as collective coordinates for the solution of the dynamical Langevin equations. The finite-range LDM, which takes into account the finite range of the nuclear forces and the diffuseness of the nuclear surface, has been used in calculations as a macroscopic model for determination of the conservative driving forces. The modified one-body mechanism of nuclear dissipation (so-called surface-plus-window dissipation) has been used to determine the friction forces.

The number of free (adjustable) parameters of the model has been reduced to a minimum. Under assumption of the surface-plus-window dissipation mechanism of nuclear viscosity, the only really variable parameter is the reduction coefficient, k_s in Eq. (14) that we have discussed above. Of course, it must be kept in mind that the definition of the scission surface adopted in the model is not unique.

The consistent calculation of the distribution parameters $\langle E_K \rangle$, $\sigma^2_{E_K}$, σ^2_M, $\langle E_K(M) \rangle$, $\sigma^2_{E_K}(M)$, and $\sigma^2_M(E_K)$ carried out on the basis of the two-dimensional MED of fission fragments shows that the stochastic approach to the fission dynamics reproduces sufficiently well the characteristics of the fission fragment MED and their dependence on the various parameters of the compound nucleus. Almost all characteristics of the MED of fission fragments depend essentially on the magnitude of the reduction coefficient of the contribution from the wall formula. Consequently, the experimental data on the variances of the fission fragment distributions can be employed together with the traditionally used $\langle E_K \rangle$ data for determination of the magnitude and mechanism of nuclear dissipation in fission.

The calculated parameters of the fission fragment MED and the mean prescission neutron multiplicity are found to be in a good quantitative agreement with the experimental data at the value of the reduction coefficient $k_s = 0.25–0.5$. This value of k_s is close to the value that was found [42] independently of fission. The value of $k_s = 1$ corresponds to the full wall-and-window formula, and to a highly overdamped collective motion, as well. It leads to considerably underestimated values of the variance of the fission fragment MED. An extension of the model for calculating the fission fragment MED in quasifission reactions induced by heavy ions is desirable.

ACKNOWLEDGMENTS

We would like to thank Dr. A. Ya. Rusanov, Dr. M. V. Mebel, and Dr. H. J. Krappe for stimulating and useful discussions, and correspondence. We are grateful to Professor M. G. Itkis for permanent support of this study. We are indebted to Dr. V. V. Mikheev for a careful reading of the manuscript. Useful discussions with Dr. G. I. Kosenko at the early stages of this work are also acknowledged. One of us (G.D.A.) wishes to thank, in particular, H. J. Krappe with whom he has had the pleasure of collaborating for the past several years and also for his encouragement without which the present paper would never have been written. This work was supported in part by the International Association of Cooperation with Scientists from the Independent States of the Former Soviet Union (Grant No. INTAS 93-1560 Ext.).

[1] H. A. Kramers, Physica (Amsterdam) **7**, 284 (1940).
[2] H. J. Krappe, in *Proceedings of the International Workshop on Dynamical Aspects of Nuclear Fission*, Smolenice, Slovakia, 1991, edited by J. Kristiak and B. I. Pustylnik (JINR, Dubna, 1992), p. 51.
[3] Y. Abe, S. Ayik, P-G. Reinhard, and E. Suraud, Phys. Rep. **275**, 49 (1996).
[4] P. Fröbrich and I. I. Gontchar, Phys. Rep. **292**, 131 (1998).
[5] H. T. Feldmeier, Rep. Prog. Phys. **50**, 915 (1987).
[6] G. D. Adeev and V. V. Pashkevich, Nucl. Phys. **A502**, 405c (1989); G. D. Adeev, I. I. Gontchar, V. V. Pashkevich, N. I. Pischasov, and O. I. Serdyuk, Fiz. Elem. Chastits At. Yadra **19**, 1229 (1988) [Sov. J. Part. Nucl. **19**, 529 (1988)].
[7] H. A. Weidenmüller, Nucl. Phys. **A471**, 1c (1987); P. Grangé,

J. O. Li, and H. A. Weidenmüller, Phys. Rev. C **27**, 2063 (1983).
[8] F. Scheuter, C. Grégoire, H. Hofmann, and J. R. Nix, Phys. Lett. **149B**, 303 (1984).
[9] Y. Abe, S. Grégoire, and H. Delagrange, J. Phys. C **47**, 4 (1986); P. Fröbrich and S. Y. Xu, Nucl. Phys. **A477**, 143 (1988).
[10] I. I. Gontchar, L. A. Litnevsky, and P. Fröbrich, Comput. Phys. Commun. **107**, 223 (1997).
[11] T. Wada, N. Carjan, and Y. Abe, Nucl. Phys. **A538**, 283c (1992); T. Wada, Y. Abe, and N. Carjan, Phys. Rev. Lett. **70**, 3538 (1993).
[12] G.-R. Tillack, R. Reif, A. Schülke, P. Fröbrich, H. J. Krappe, and H. G. Reusch, Phys. Lett. B **296**, 296 (1992); G.-R. Tillack, *ibid.* **278**, 403 (1992).
[13] G. I. Kosenko, I. I. Gontchar, N. I. Pischasov, and O. I. Serdyuk, Yad. Fiz. **55**, 920 (1992) [Sov. J. Nucl. Phys. **55**, 514 (1992)].
[14] J. Bao, Y. Zhuo, and X. Wu, Z. Phys. A **352**, 321 (1995).
[15] G. I. Kosenko, I. G. Cagliari, and G. D. Adeev, Yad. Fiz. **60**, 404 (1997) [Phys. At. Nucl. **60**, 334 (1997)]; G. I. Kosenko, D. V. Vanin, and G. D. Adeev, *ibid.* **61**, 416 (1998) [**61**, 356 (1997)].
[16] D. V. Vanin, G. I. Kosenko, and G. D. Adeev, Phys. Rev. C **59**, 2114 (1999); D. V. Vanin, P. N. Nadtochy, G. I. Kosenko, and G. D. Adeev, Yad. Fiz. **63**, 1957 (2000) [Phys. At. Nucl. **63**, 1865 (2000)].
[17] J. R. Nix and W. J. Swiatecki, Nucl. Phys. **71**, 1 (1965); J. R. Nix, Nucl. Phys. **A130**, 241 (1969).
[18] O. I. Serdyuk, G. D. Adeev, I. I. Gontchar, V. V. Pashkevich, and N. I. Pischasov, Yad. Fiz. **46**, 710 (1987) [Sov. J. Nucl. Phys. **46**, 399 (1987)]; G. Saupe, O. I. Serduyk, G. D. Adeev, and V. V. Pashkevich, *ibid.* **48**, 42 (1988) [**48**, 26 (1988)].
[19] M. Brack, J. Damgaard, A. S. Jensen, H. C. Pauli, V. M. Strutinsky, and C. Y. Wong, Rev. Mod. Phys. **44**, 320 (1972).
[20] H. C. Pauli, Phys. Rep. **7**, 35 (1973).
[21] V. M. Strutinsky, N. Ya. Lyashchenko, and N. A. Popov, Nucl. Phys. **46**, 639 (1962).
[22] S. Cohen and W. J. Swiatecki, Ann. Phys. (N.Y.) **22**, 406 (1963).
[23] H. C. Pauli, Nukleonika **20**, 601 (1975); T. Ledergerber and H. C. Pauli, Nucl. Phys. **A207**, 1 (1973).
[24] V. M. Strutinsky, Zh. Éksp. Teor. Fiz. **18**, 1305 (1964) [JETP **45**, 1900 (1963)].
[25] K. T. R. Davies and A. J. Sierk, Phys. Rev. C **31**, 915 (1985).
[26] R. K. Gupta, W. Scheid, and W. Greiner, Phys. Rev. Lett. **35**, 353 (1975); W. Greiner, M. Ivascu, D. Poenaru, and A. Sandulescu, in *Treatise on Heavy Ion Science*, edited by D. A. Bromley (Plenum, New York, 1988), Vol. 8, p. 641.
[27] H. C. Pauli, T. Ledergerber, and M. Brack, Phys. Lett. **34B**, 264 (1971).
[28] T. Ledergerber, H. C. Pauli, and Y. Yariv, Nucl. Phys. **A280**, 241 (1977).
[29] V. V. Voevodin, *Linear Algebra* (Fizmatgiz, Moscow, 1974) [in Russian]; J. H. Wilkinson, *The Algebraic Eigenvalue Problem* (Oxford University Press, New York, 1965).
[30] A. V. Ignatyuk, *Statistical Properties of Excited Nuclei* (Energoatomizdat, Moscow, 1983) [in Russian]; translated as IAEA Report No. INDC (CCP) 233/L 1985 (unpublished); R. G. Stokstad, in *Treatise on Heavy Ion Science*, edited by D. A. Bromley (Plenum, New York, 1985), Vol. 3, p. 83.
[31] A. V. Ignatyuk, M. G. Itkis, V. N. Okolovich, G. N. Smirenkin, and A. S. Tishin, Yad. Fiz. **21**, 1185 (1975) [Sov. J. Nucl. Phys. **21**, 612 (1975)].
[32] J. Marten and P. Fröbrich, Nucl. Phys. **A545**, 854 (1992).
[33] H. J. Krappe, J. R. Nix, and A. J. Sierk, Phys. Rev. C **20**, 992 (1979).
[34] A. J. Sierk, Phys. Rev. C **33**, 2039 (1986).
[35] A. Bohr and B. Mottelson, *Nuclear Structure* (Benjamin, New York, 1975).
[36] J. O. Newton, Fiz. Elem. Chastits At. Yadra **21**, 821 (1990) [Sov. J. Part. Nucl. **21**, 349 (1990)].
[37] C. Guet, E. Strumberger, and M. Brack, Phys. Lett. B **205**, 427 (1988).
[38] M. Brack, C. Guet, and H. B. Håkonsson, Phys. Rep. **123**, 275 (1985).
[39] H. J. Krappe, Phys. Rev. C **59**, 2640 (1999).
[40] K. T. R. Davies, A. J. Sierk, and J. R. Nix, Phys. Rev. C **13**, 2385 (1976); J. R. Nix and A. J. Sierk, Nucl. Phys. **A428**, 161c (1984).
[41] A. A. Seregin, Yad. Fiz. **55**, 2639 (1992) [Sov. J. Nucl. Phys. **55**, 1473 (1992)].
[42] J. R. Nix and A. J. Sierk, in *Proceedings of the International School–Seminar on Heavy Ion Physics*, Dubna, USSR, 1986, edited by M. I. Zarubina and E. V. Ivashkevich (JINR, Dubna, 1987), p. 453; J. R. Nix, Nucl. Phys. **A502**, 609 (1989).
[43] J. R. Nix and A. J. Sierk, in *Proceedings of the Sixth Adriatic Conference on Nuclear Physics: Frontiers of Heavy Ion Physics*, Dubrovnik, Yugoslavia, 1987, edited by N. Cindro, R. Caplar, and W. Greiner (World Scientific, Singapore, 1990), p. 333.
[44] A. J. Sierk and J. R. Nix, Phys. Rev. C **21**, 982 (1980).
[45] J. Blocki, Y. Boneh, J. R. Nix, J. Randrup, M. Robel, A. J. Sierk, and W. J. Swiatecki, Ann. Phys. (N.Y.) **113**, 330 (1978).
[46] J. J. Griffin and M. Dworzecka, Nucl. Phys. **A455**, 61 (1986).
[47] J. Randrup and W. J. Swiatecki, Nucl. Phys. **A429**, 105 (1984).
[48] J. Blocki, H. T. Feldmeier, and W. J. Swiatecki, Nucl. Phys. **A459**, 145 (1986); J. Blocki, R. Planeta, J. Brzychczyk, and K. Grotowski, Z. Phys. A **341**, 307 (1992).
[49] W. J. Swiatecki, in *Proceedings of Niels Bohr Centennial Symposium on Semiclassical Description of Atomic and Nuclear Collisions*, Copenhagen, edited by J de Boer and J. Bang, (North Holland, Amsterdam, 1985), p. 281.
[50] S. Pal and T. Mukhopadhy, Phys. Rev. C **57**, 210 (1998); T. Mukhopadhy and S. Pal, *ibid.* **56**, 296 (1997).
[51] V. Weisskopf, Phys. Rev. **52**, 295 (1937).
[52] A. S. Iljinov, M. V. Mebel, N. Bianchi, E. De Sanotis, C. Guaraldo, V. Lucherini, V. Muccifora, E. Polli, A. R. Reolon, and P. Rossi, Nucl. Phys. **A543**, 517 (1992).
[53] N. D. Mavlitov, P. Fröbrich, and I. I. Gontchar, Z. Phys. A **342**, 195 (1992).
[54] C. Bhattacharya, S. Bhattacharya, and K. Krishan, Phys. Rev. C **53**, 1012 (1996); A. K. Dhara, K. Krishan, C. Bhattacharya, and S. Bhattacharya, *ibid.* **57**, 2453 (1998).
[55] D. Hilscher and H. Rossner, Ann. Phys. (N.Y.) **17**, 471 (1992); D. J. Hinde, D. Hilscher, and H. Rossner, Nucl. Phys. **A502**, 497c (1989).
[56] D. J. Hinde, D. Hilscher, H. Rossner, B. Gebauer, M. Leh-

mann, and M. Wilpert, Phys. Rev. C **45**, 1229 (1992).
[57] G. G. Chubaryan, M. G. Itkis, S. M. Lukyanov, V. N. Okolovich, Yu. E. Penionzkevich, A. Ya. Rusanov, V. S. Salamatin, and G. N. Smirenkin, Yad. Fiz. **56**, 3 (1993) [Phys. At. Nucl. **56**, 286 (1993)].
[58] M. G. Itkis, S. M. Lukyanov, V. N. Okolovich, Yu. E. Penionzkevich, A. Ya. Rusanov, V. S. Salamatin, G. N. Smirenkin, and G. G. Chubaryan, Yad. Fiz. **52**, 23 (1990) [Sov. J. Nucl. Phys. **52**, 15 (1990)].
[59] A. Ya. Rusanov, M. G. Itkis, and V. N. Okolovich, Yad. Fiz. **60**, 773 (1997) [Phys. At. Nucl. **60**, 683 (1997)].
[60] M. G. Itkis, Yu. Ts. Oganessian, G. G. Chubarian, V. S. Salamatin, A. Ya. Rusanov, and V. N. Okolovich, in *Proceedings of the XV EPS Conference on Low Energy Nuclear Dynamics (LEND-95)*, St. Petersburg, 1995, edited by Yu. Ts. Oganessian, R. Kalpakchieva, and W. von Oertzen (World Scientific, Singapore, 1995), p. 177.
[61] F. Gönnenwein, in *Nuclear Fission Process*, edited by C. Wagemans (CRC Press, Boca Raton, FL, 1991), p. 287.
[62] M. G. Itkis and A. Ya. Rusanov, Fiz. Elem. Chastits At. Yadra **29**, 398 (1998) [Phys. Part. Nucl. **29**, 160 (1998)].
[63] K. T. R. Davies, R. A. Managan, J. R. Nix, and A. J. Sierk, Phys. Rev. C **16**, 1890 (1977).
[64] S. K. Samaddar, D. Sperber, M. Zielińska-Pfabé, and M. I. Sobel, Phys. Scr. **25**, 517 (1982).
[65] K. T. R. Davies and J. R. Nix, Phys. Rev. C **14**, 1977 (1976).
[66] U. Brosa, S. Grossmann, and A. Müller, Phys. Rep. **197**, 167 (1990).
[67] V. E. Viola, K. Kwiatkowski, and M. Walker, Phys. Rev. C **31**, 1550 (1985); V. E. Viola, Nucl. Data Tables **A1**, 391 (1966).
[68] P. Fong, *Statistical Theory of Nuclear Fission* (Gordon and Breach, New York, 1969).
[69] T. Wada, in *Proceedings of the Second Tours Symposium on Nuclear Physics*, Tours, 1994, edited by H. Utsunomiya, M. Ohta, J. Galin, and G. Munzenberg (World Scientific, Singapore, 1995), p. 470; Y. Abe, in *Proceedings of the Third IN2P3-RIKEN Symposium on Heavy Ion Collisions*, Tokyo, 1994, edited by T. Motobayashi, N. Frascaria, and M. Ishihara (World Scientific, Singapore, 1995), p. 123.
[70] G. Kendall and A. Stuart, *The Advaced Theory of Statistics*, (Griffin, London, 1958), Vol. 1.
[71] M. G. Itkis, V. N. Okolovich, and G. N. Smirenkin, Nucl. Phys. **A502**, 243c (1989); M. G. Itkis, V. N. Okolovich, A. Ya. Rusanov, and G. N. Smirenkin, Fiz. Elem. Chastits At. Yadra. **19**, 702 (1988) [Sov. J. Part. Nucl. **19**, 301 (1988)].
[72] M. G. Itkis, V. N. Okolovich, A. Ya. Rusanov, and G. N. Smirenkin, Yad. Fiz. **41**, 1109 (1985) [Sov. J. Nucl. Phys. **41**, 709 (1985)].
[73] K. Siewek-Wilczyńska, J. Wilczyński, R. H. Siemssen, and H. W. Wilschut, Phys. Rev. C **51**, 2054 (1995).
[74] J. Wilczyński, K. Siwek-Wilczyńska, and H. W. Wilschut, Phys. Rev. C **54**, 325 (1996).
[75] A. Saxena, A. Chatterjee, R. K. Choudhury, S. S. Kapoor, and D. M. Nadkarni, Phys. Rev. C **49**, 932 (1994).